EARTHQUAKE ENGINEERING AND STRUCTURAL DYNAMICS
Earthquake Engng. Struct. Dyn. **27**, 1277–1289 (1998)

DESIGN OF $\mathbf{H}_\infty$ OUTPUT FEEDBACK CONTROLLERS FOR THE AMD BENCHMARK PROBLEM

SCOTT E. BRENEMAN† AND H. ALLISON SMITH*,‡
Department of Civil Engineering, Stanford University, Stanford, CA 94305-4020, U.S.A.

SUMMARY

This paper outlines a general approach for the design of $\mathbf{H}_\infty$ dynamic output feedback controllers and applies this method to designing controllers for the Active Mass Driver (AMD) benchmark problem. The example controllers designed for this problem use acceleration output feedback of the structure coupled with the additional actuator sensors and ground motion sensor. Some of the key choices made by a control designer using this method are discussed and evaluated with example controllers. Several sets of controllers are developed to evaluate the sensitivity of controller effectiveness to the choice of regulator response quantities, the choice of feedback quantities, and the choice of when to apply model reduction. Results show that for this design approach the best controller effectiveness is achieved by choosing to regulate the structural accelerations and displacements with the controller acceleration and command signal. In addition, the sensitivity of the dynamic controllers to the removal of available sensors is investigated, showing that the performance of the dynamic controllers for the nominal AMD model are insensitive to which sensors are available.

KEY WORDS: output feedback; active structural control; benchmark problem; seismic control

INTRODUCTION

In recent years considerable research activity has occurred in the area of active structural control for civil structures. Although significant progress has been made towards the design of feasible and practically realizable controllers for earthquake engineering applications, assessing the overall status of this research field has been difficult because of the relatively wide variability in control objectives. The benchmark problems presented by Spencer *et al.*[1] attempt to enforce a specific set of objectives, thus providing a common ground from which various control design methods may be tested.

This research employs total acceleration measurements of selected degrees of freedom as the feedback quantity for the controllers. Accelerometers are one of the most commonly employed sensors on civil structures in seismic zones, and direct use of accelerations requires no additional signal processing to obtain a relevant measurement for feedback. Acceleration feedback has beem employed in civil structural control in several recent research efforts. Acceleration feedback was introduced for $\mathbf{H}_2$ control by Spencer *et al.*[2] using an inner feedback loop. More recently, Jabbari *et al.*[3] employed acceleration feedback $\mathbf{H}_\infty$ control to attenuate structural response to seismic loads for linear time invariant systems. Additional acceleration feedback $\mathbf{H}_\infty$ control research for civil structures has been performed by Dyke *et al.*[4]

* Correspondence to: H. Allison Smith, Department of Civil Engineering, Stanford University, Stanford, CA 94305-4020, U.S.A.
† Ph.D. Candidate
‡ Associate Professor

Contract/grant sponsor: National Science Foundation; Contract/grant number: BCS-9058316
Contract/grant sponsor: Office of Naval Research
Contract/grant sponsor: Naval Research Lab.; Contract/grant number: N00014-94-1-0554

CCC 0098–8847/98/111277–13$17·50

Received 10 August 1997
Revised 2 December 1997

Recent research has shown $\mathbf{H}_\infty$ control to be particularly effective for civil structures.[5] For $\mathbf{H}_\infty$ control methods, Stoustrup and Niemann[14] developed controllers for Linear Time-Invariant (LTI) systems that do not include the acceleration feedback case. Gu and Misra[6] also designed controllers for LTI systems with the added constraint that the number of inputs equal the number of measured outputs. Peres *et al.*[7] used linear matrix inequalities to obtain robust static output feedback $\mathbf{H}_\infty$ controllers. Finally, Kose *et al.*[8] developed robust static output feedback $\mathbf{H}_\infty$ controllers for civil structures based on the framework for static output feedback control for LTI systems developed by Skelton *et al.*[9]

This paper presents the application of the $\mathbf{H}_\infty$ control theory to designing controllers for the Active Mass Driver (AMD) presented by Spencer *et al.*[1] Controllers are designed using standard $\mathbf{H}_\infty$ dynamic output feedback control synthesis tools available in the MATLAB's LMI Control Toolbox. Using this approach, several of the key choices made by a designer during the synthesis process are investigated, including the definition of the regulated output, when to perform model reduction, and the effect of available sensors. The next section reviews the $\mathbf{H}_\infty$ output feedback control approach. Following the review is a description of the design model used in this work and then a section presenting and comparing the example controllers.

$\mathbf{H}_\infty$ OUTPUT FEEDBACK CONTROL

This section reviews output feedback control and the $\mathbf{H}_\infty$ theory used in this research. The controllers considered in this study are designed using a continuous-time $\mathbf{H}_\infty$ controller approach, then converted to discrete controllers for simulation with the benchmark models. The controllers are developed from the general two-port state-space design model given in equations (1)–(3), which includes the structural model, known actuator dynamics, and all input and output magnitude and frequency weightings:

$$\dot{\mathbf{x}}(t) = \mathbf{A}\mathbf{x}(t) + \mathbf{B}_u u(t) + \mathbf{B}_w \mathbf{w}(t) \tag{1}$$

$$\mathbf{z}(t) = \mathbf{C}_z \mathbf{x}(t) + \mathbf{D}_{zu} u(t) + \mathbf{D}_{zw} \mathbf{w}(t) \tag{2}$$

$$\mathbf{y}(t) = \mathbf{C}_y \mathbf{x}(t) + \mathbf{D}_{yu} u(t) + \mathbf{D}_{yw} \mathbf{w}(t) \tag{3}$$

The matrix $\mathbf{A}$ represents the plant matrix, while $\mathbf{B}_u$ maps the control inputs, $u(t)$, to the state space, and $\mathbf{B}_w$ maps the external excitations, $\mathbf{w}(t)$, into the system states. The regulated outputs are given by $\mathbf{z}(t)$ from the mapping matrices $\mathbf{C}_z$, $\mathbf{D}_{zu}$, and $\mathbf{D}_{zw}$. Similarly, the available sensor measurements are given by $\mathbf{y}(t)$ as defined by the matrices $\mathbf{C}_y$, $\mathbf{D}_{yu}$, and $\mathbf{D}_{yw}$.

This research develops continuous linear output feedback controllers of the form given in equations (4) and (5),

$$\dot{\mathbf{x}}_c(t) = \mathbf{A}_c \mathbf{x}_c(t) + \mathbf{B}_c \mathbf{y}(t) \tag{4}$$

$$u(t) = \mathbf{C}_c \mathbf{x}_c(t) + \mathbf{D}_c \mathbf{y}(t) \tag{5}$$

where $\mathbf{x}_c(t)$ is the state vector of the dynamic controller and $\mathbf{A}_c$, $\mathbf{B}_c$, $\mathbf{C}_c$ and $\mathbf{D}_c$ are the state description of the dynamic controller. The control design completed with a continuous-time model of both the system and feedback loop does not explicitly account for the time delay and discretization error introduced by the digital implementation of the controller, nor potential actuator saturation. The design model and dynamic feedback control system can then be converted into a closed-loop model of the form

$$\dot{\hat{\mathbf{x}}}(t) = \mathbf{A}_{cl} \hat{\mathbf{x}}(t) + \mathbf{B}_{cl} \mathbf{w}(t) \tag{6}$$

$$\mathbf{z}(t) = \mathbf{C}_{cl} \hat{\mathbf{x}}(t) + \mathbf{D}_{cl} \mathbf{w}(t) \tag{7}$$

where the transfer function matrix of this linear model from the external excitations, $\mathbf{w}(t)$, to the regulated output, $\mathbf{z}(t)$, is written as

$$\mathbf{T}_{zw}(s) = \mathbf{C}_{cl}(s\mathbf{I} - \mathbf{A}_{cl})^{-1} \mathbf{B}_{cl} + \mathbf{D}_{cl} \tag{8}$$

In general, $\mathbf{H}_\infty$ control methods minimize the maximum amplification of the transfer function matrix between the disturbance input, $\mathbf{w}(t)$, and the regulated output, $\mathbf{z}(t)$. The infinity norm of linear certain dynamic systems can be defined as the maximum gain of the transfer function $\mathbf{T}_{zw}$ as follows:

$$\|\mathbf{T}_{zw}\|_\infty \doteq \sup_{\omega \in \Re} \bar{\sigma}[\mathbf{T}_{zw}(\mathrm{j}\omega)] = \gamma \tag{9}$$

where $\bar{\sigma}$ is the maximum singular value of the matrix at a given frequency ω. Minimizing the infinity norm (γ) of a system is equivalent to minimizing the worst-case Root-Mean Square (RMS) gain of the system, bounding the transfer function over the entire family of disturbance inputs, $\mathbf{w}(t)$.

The $\mathbf{H}_\infty$ controller design is approached from Linear Matrix Inequality (LMI) methods which are particularly well suited for solution with modern computational tools, such as the LMI control toolbox in MATLAB or other software packages. For the closed-loop system described in equations (6) and (7), the infinity norm of a stable system is the minimum γ that satisfies the following LMI:

$$\left[\begin{array}{c|c} \mathbf{A}_{\mathrm{cl}}\mathbf{P} + \mathbf{P}\mathbf{A}_{\mathrm{cl}} + \mathbf{C}_{\mathrm{cl}}^{\mathrm{T}}\mathbf{C}_{\mathrm{cl}} & \mathbf{P}\mathbf{B}_{\mathrm{cl}} \\ \hline \mathbf{B}_{\mathrm{cl}}^{\mathrm{T}}\mathbf{P} & \mathbf{D}_{\mathrm{cl}}^{\mathrm{T}}\mathbf{D}_{\mathrm{cl}} - \gamma^2\mathbf{I} \end{array}\right] \leqslant 0 \tag{10}$$

where $\mathbf{P}$ is a symmetric positive-definite matrix and the $\leqslant 0$ signifies that the composite matrix is negative semi-definite. Discussions on the solution of LMI for cases of $\mathbf{H}_\infty$ controller synthesis can be found in Doyle *et al.*[10] and Boyd *et al.*[11] This research solves the controller synthesis problems using the LMI Control Toolbox available for the MATLAB environment.

Controller design model

Using this approach for controller synthesis, effective controller design is reduced to intelligently forming the two-port state-space design model in equations (1)–(3). To accomplish this objective, a control system designer needs to make a variety of choices, including choosing what is modelled in the input and output description of the system, the frequency and magnitude weighting of the excitations and regulated output, and when and how to impose constraints on the order of the dynamic feedback controller.

For our controller design, the external input, $\mathbf{w}(t)$, to the system is comprised of the external ground motion excitation, $\ddot{x}_{\mathrm{g}}(t)$, sensor noise disturbance, $\mathbf{v}_y$, and a command signal disturbance, $\mathbf{v}_u$. Both the ground motion excitation acceleration and the sensor noise are explicitly discussed and described in the definition of the AMD benchmark problem in Spencer *et al.*[1] The command signal disturbance is added to account for noise introduced to the command signal by the discrete digital implementation of the continuous controller and potential noise in the actuator response to the command signal. A block diagram of the design model showing these excitations and disturbances to the system as well as the components of the regulated output can be seen in Figure 1.

The sensor measurements, $\mathbf{y}(t)$, made available for the controllers in these designs are the six primary sensor measurements available in the active mass driver control system, namely the actuator displacement and acceleration, the three structural accelerations, and the ground motion excitation. The inclusion of the ground motion measurement creates a feed-forward loop; however, the suggested controller design methods needs no special modification to handle the feed-forward loop.

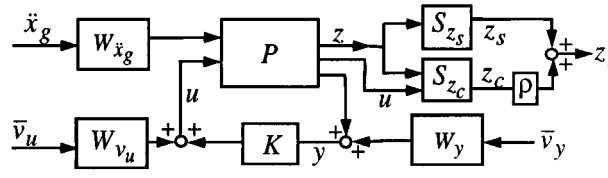

Figure 1. Schematic of control design model

Sensor and command signal noise

The sensor noise for the evaluation of the benchmark model is defined to be band-limited white noise. Because of this noise model, the sensor noise weighting, $\mathbf{W}_{v_y}$, was chosen to be constant at all frequencies. The magnitude of the weighting, was chosen as 0·01 which is the RMS magnitude of the random noise signals in the evaluation model. The command signal disturbance is also weighted by a constant, 0·005 over all frequencies. The weighting of 0·005 was chosen as this is a few factors greater than the 0·00146 discretization interval of the digital to analog converter in the controller. The magnitude of the weights of the sensor noise and the command signal disturbance was modified for a few sample controller designs with the resulting simulations showing the controller effectiveness fairly insensitive to changes in $\mathbf{W}_{v_u}$ and $\mathbf{W}_{v_u}$ of an order of magnitude or less. All of the controllers presented in the following discussion are based on these weights.

Ground motion excitation weighting

To account for the frequency content of the ground motion acceleration, the excitation weighting, $\mathbf{W}_{\ddot{x}_g}$, is set to a Kanai–Tajimi filter with the dominant frequency, ω_g, of 120 rad/sec and the damping coefficient, ζ_g, of 0·90. This filter was chosen as it provides a fairly constant level of excitation for all frequencies below 120 rad/sec and diminishes at higher frequencies. The singular value plot of this design filter is shown in Figure 2 with example singular value plots of Kanai–Tajimi filters that cover the range of ω_g from 20 to 120 rad/sec, each at the minimum ζ_g value of 0·3.

Regulated output

The regulated output of the design models for the benchmark models is formed by first appending the controller command signal, u, to the full regulated output, $\mathbf{z}$, as defined in Spencer *et al.*[1]

$$\mathbf{z} = [x_1 \;\; x_2 \;\; x_3 \;\; x_m \;\; \dot{x}_1 \;\; \dot{x}_2 \;\; \dot{x}_3 \;\; \dot{x}_m \;\; \ddot{x}_{a1} \;\; \ddot{x}_{a2} \;\; \ddot{x}_{a3} \;\; \ddot{x}_{am} \;\; u]^{\mathrm{T}} \tag{11}$$

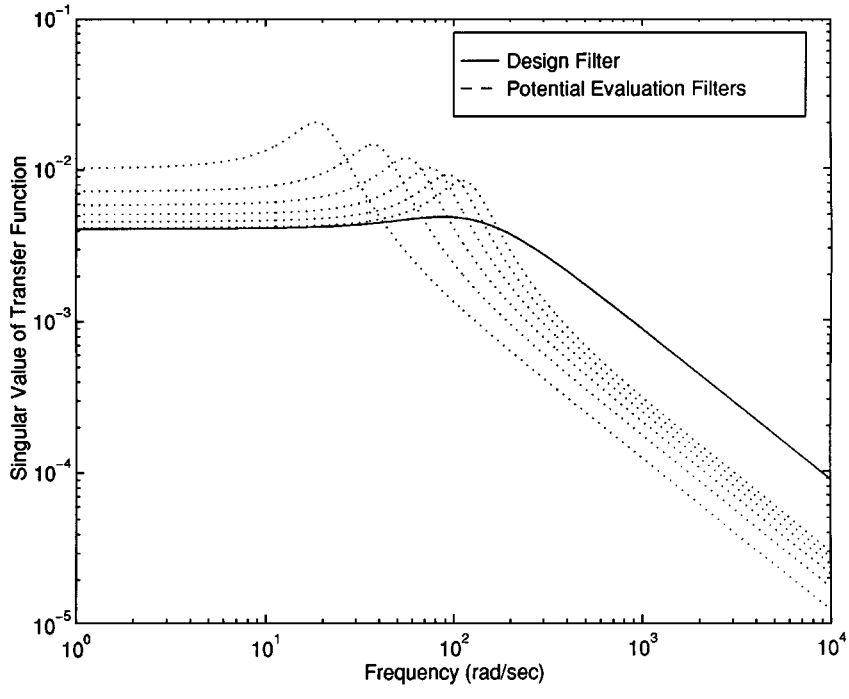

Figure 2. Earthquake excitation weighting, $\mathbf{W}_{\ddot{x}_g}$

Each element of the augmented output is the normalized by a reference value to keep the magnitudes roughly equivalent. For the AMD benchmark model the structure and actuator displacement components of z are normalized by 1·13 cm, the velocities by 47·9 cm/sec, and accelerations by 1·79 g. These values are the peak response values for the third floor during an uncontrolled response to the El Centro earthquake record. The command signal, u, is normalized by a reference value of 1 V.

As the augmented regulated output contains both structural response measures and controller effort measures, two secondary output vectors are formed to assist in the design. The first regulated output vector, $\mathbf{z}_s = \mathbf{S}_{z_s}\mathbf{z}$, is formed as a measure of the structural response and can be taken as any combination of structural performance characteristics of interest. The matrix $\mathbf{S}_{z_s}$ is defined to choose which of the structural response quantities (displacements, velocities, or accelerations) are to be regulated by the controller. The examples shown later include regulating the structural displacements, velocities, and absolute accelerations individually, as well as combinations of two of these three quantities. The second measure of performance, $\mathbf{z}_c = \mathbf{S}_{z_c}\mathbf{z}$, is formed to represent the controller effort needed by the closed-loop system and can be a combination of the actuator command signal, u, actuator displacement, actuator velocity and actuator acceleration of the AMD.

To perform the $\mathbf{H}_\infty$ control synthesis, a single regulated output is used. This regulated output, $\mathbf{z}_r$, is defined as

$$\mathbf{z}_r = \mathbf{z}_s + \rho\mathbf{z}_c \tag{12}$$

where ρ is a design parameter. This definition is chosen as it allows direct exploration of the trade-off between the structural response attenuation and the controller effort required. Ideally, we desire a large structural response attenuation (small $\mathbf{z}_s$) with minimal control effort applied (small $\mathbf{z}_c$). The combination of a measure of the disturbance rejection with a measure of controller effort can be seen in many controller design methods. A familiar example of this method is in the quadratic cost function of the standard Linear Quadratic Regulator.

$$J = \int_0^\infty (\mathbf{x}^T\mathbf{Q}\mathbf{x} + \rho u^T u)\,dt \tag{13}$$

The ρ in our regulated output plays the same role as the ρ in LQR design, that of weighting the relative cost of the system response reduction with the cost of the control effort. Other methods are available in $\mathbf{H}_\infty$ control and related theories that take a more explicit method to examine this and other multi-objective design problems. Rotea and Prasanth[12] present one such method and include numerous references of work in this area.

Model reduction requirements

Another important aspect of the controller design is the ability to produce controllers of limited complexity. For the dynamic output feedback controllers, the complexity is characterized by the number of state variables in the controller state vector, $\mathbf{x}_c$. The evaluation model provided for the AMD model is 28th order, while the benchmark problem limits the dynamic order of candidate controllers to 12 states or less. The $\mathbf{H}_\infty$ controller design used in this study creates controllers of the same order as the design model, including both the plant and all frequency weightings. Hence, model reduction is unavoidable when using this design method. The designer can apply model reduction at various stages to generate controllers of the appropriate size. One option is to reduce the initial plant size so that, when augmented with the frequency weightings, the design model is of the desired size. A second option is to augment the plant model with the frequency weighting and then perform model reduction. As a third option, the designer can create high-order controllers for the unreduced, frequency weighted plant model and then reduce the resulting controllers to the desired order. This method may create better controllers while requiring more computational effort during the synthesis stages.

EXAMPLE CONTROLLERS AND RESULTS

The design model and $\mathbf{H}_\infty$ controller synthesis methods have been used to examine effective means of generating controllers for the benchmark problems. First, we examine the choice of what to regulate in the structural response measure, $\mathbf{z}_s$, by varying the output mapping matrix $\mathbf{S}_{z_s}$. Following this analysis, we turn our attention to the control effect measure, $\mathbf{z}_c$, and the accompanying mapping matrix, $\mathbf{S}_{z_c}$. Third, we examine the effect of implementing the model reduction techniques at the various stages of design as previously described. Finally, we remove some of the sensors available to the controller and discuss the robustness of the controllers under these conditions.

In each of these sections, the disturbance input excitation weightings are not changed from the values already discussed. To reiterate, the earthquake excitation weighting, $\mathbf{W}_{\ddot{x}_g}$, is a Kanai–Tajimi filter with $\omega_g = 120$ rad/sec and $\zeta_g = 0{\cdot}9$. The sensor noise weighting, $\mathbf{W}_{v_y}$, is a constant of 0·01 and the command signal disturbance weighting, $\mathbf{W}_{v_u}$, is a constant of 0·005.

The AMD benchmark control problem evaluates controllers by simulating candidate controllers using two historical earthquake records, from the El Centro and the Hachinohe earthquakes, and simulating the controlled system with a stochastic ground motion excitation. The spectral characteristics of the excitation are defined with a Kanai–Tajimi filter with a dominant natural frequency, ω_g, in the range from 20 to 120 rad/sec and a damping factor or shape factor, ζ_g, in the range from 0·3 to 0·75, with a RMS value of the ground motions acceleration at a constant of 0·12 g.

The stochastic response indices J1 and J2 are the maximum normalized RMS response of the inter-storey drifts and the structural accelertions. J3, J4, and J5 are the maximum normalized RMS response of the actuator displacement, actuator velocity and absolute actuator acceleration, respectively. These indices are defined as the maximum RMS response value over the range of allowable excitation filters. The stochastic response performance indices, J1–J5, are calculated by simulating the full evaluation model of the controller for 300 sec. In this research, the worst-case Kanai–Tajimi input parameters, ω_g and ζ_g, were found for the closed-loop continuous system. As these closed-loop worst-case parameters are very close to the open-loop worst-case parameters of $\omega_g = 37{\cdot}3$ rad/sec and $\zeta_g = 0{\cdot}3$, the controller simulation results presented are from simulation with the full evaluation model at the open-loop worse-case parameters. The performance indices J6–J10 are for the same structural response values as J1–J5 but for the peak response to simulation with the two scaled historical earthquake records. The AMD benchmark model also prescribes constraints on the actuator effort by requiring the worst-case RMS response to be less than 3 cm for the actuator displacement, less than 2 g for the actuator acceleration and less than 1 V for the controller command signal.The similar peak constraints to the historical earthquake simulations are 9 cm, 6 g and 3 V.

Structural response regulation

We have examined the choice of what to regulate for the structural response measure, $\mathbf{z}_s$, by using several values of $\mathbf{S}_{z_s}$ and simulating the resulting controllers with the El Centro and Hachinohe earthquakes. The possibilities explicitly considered and presented are for regulating the structural displacements(d), velocities(v), and accelerations(a) and then combinations of the above taken two at a time. For each of the cases examined in this section, the controller effort measure selected for $\mathbf{z}_c$ is strictly the command signal u. Six sets of controllers were generated and simulated for this examination. Controller Set 1 is comprised of controllers for which $\mathbf{z}_s$ is the sum of the normalized structural displacements. Controller Sets 2 and 3 are designed to regulate the structural velocity and absolute accelerations, respectively. For each set, a series of ρ values between 100 and 0·1 are used to generate controllers over the entire range of the structural response and controller effort trade-off curves.

For comparing the properties of these controller sets, Figure 3 plots the structural response performance indices J6 and J7 versus the actuator response indices J8 and J10. Examining the plot of the structural drift index, J6, versus the actuator displacement index, J8, we see a classic trade-off curve with decreasing marginal gains in structural response at higher actuator effort. The plots of the storey drift, J6, and storey acceleration,

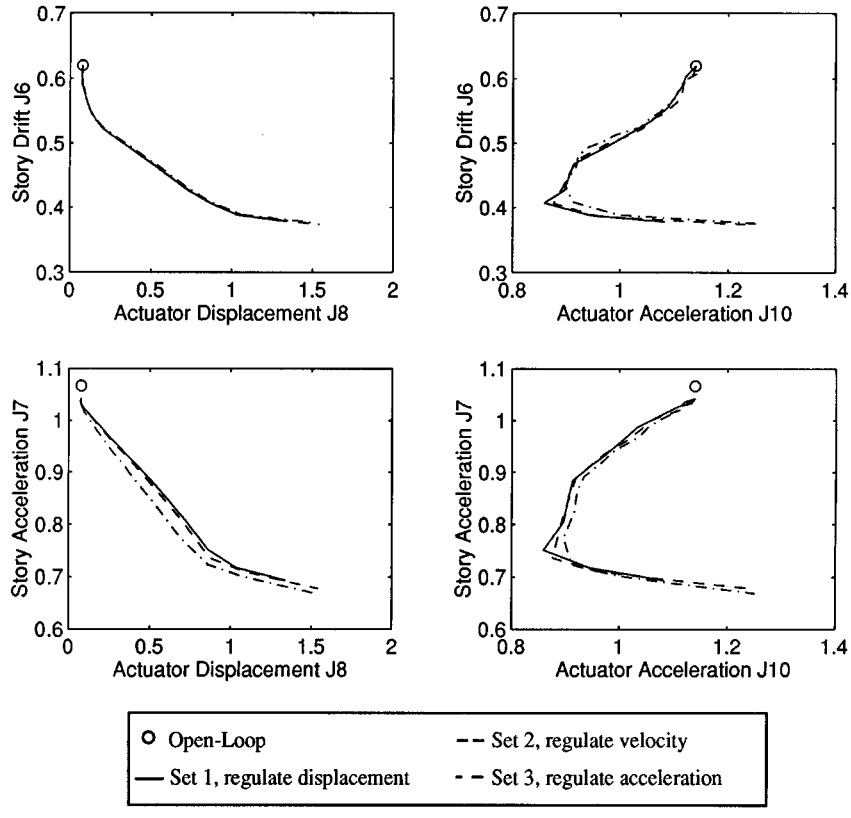

Figure 3. Investigation of $\mathbf{S}_{z_s}$, structural response regulation

J7, versus actuator acceleration, J10, have an interesting feature of drifting away from the open-loop point towards the origin and then transitioning to a trade-off type curve below J6 = 0·4 and J7 = 0·75. This phenomena occurs because the actuator is located on the third floor, such that its absolute acceleration is a sum of the 3rd floor acceleration and the relative acceleration of the actuator to the floor. At low levels of control, the net result of actuation reduces the total acceleration felt by the actuator; however, at higher levels of control the relative acceleration between the actuator and floor dominates.

From this comparison, we see no significant change between the controller sets in the relationship for peak interstorey drift versus actuator displacement. Controller Set 3, regulating accelerations, produces significantly lower storey accelerations for a given actuator displacement value, but this reduction in storey accelerations is at the cost of higher actuator accelerations. The trend follows very closely to the observations suggested by Dyke *et al.*[4] At high levels of actuator effort, the storey acceleration versus actuator accelerations curves are nearly identical.

A similar comparison for the additional sets of controllers are given in Figure 4. Controller Set 4 has the regulated structural output as the structural displacements and structural velocities. Controller Set 5 regulates the structural displacements and accelerations while controller Set 6 regulates the structural velocities and accelerations. The two observations made from Figure 3 are also true in this comparison. The structural drift versus actuator diplacement curve is only negligibly affected as is the structural acceleration versus actuator acceleration at high levels of structure attenuation. Controller Set 5 performs well in reducing the structural drifts and accelerations at a given level of actuator displacement, with the cost of increased actuator accelerations.

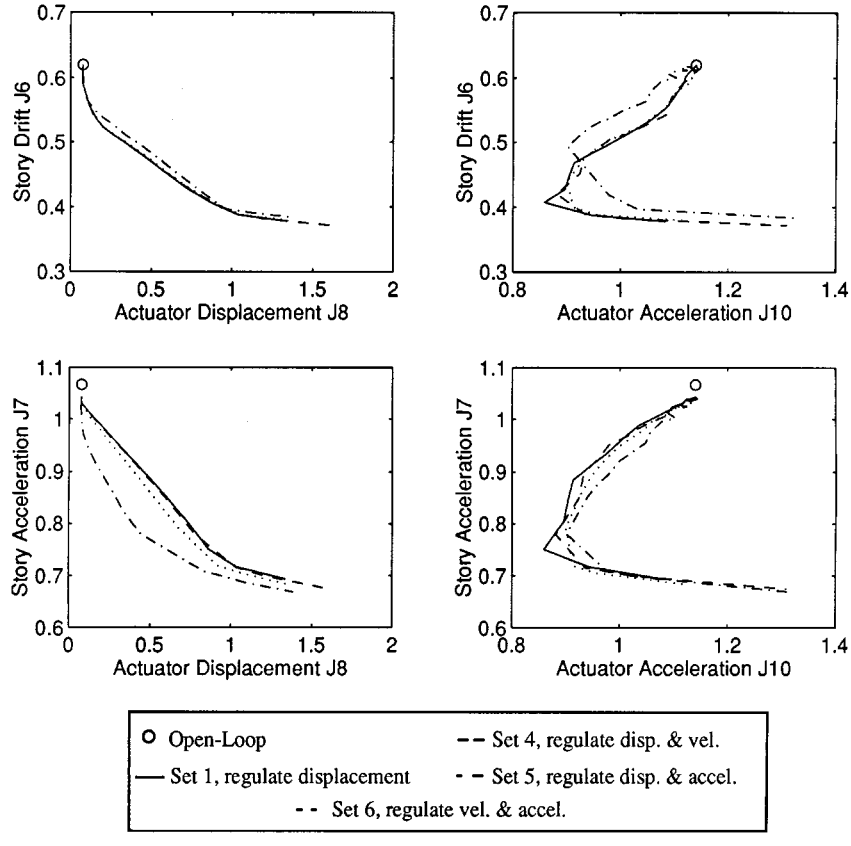

Figure 4. Investigation of $\mathbf{S}_{z_s}$, structural response regulation

Specific performance values for both the random earthquake excitation and the historic records are presented in Table I. The controllers presented in the table were chosen to have roughly the same reduction of the interstorey drift (J6 $\approx$ 0·388). This level was chosen as most of the controllers are near their full effectiveness without having too high of an actuator acceleration.

Controller effort regulation

A second investigation was made to determine the effect of the choice of the measure of controller effort, $\mathbf{z}_c$. The base controllers for this investigation is controller Set 1 which regulates the structural displacement response and the controller command signal. Three new sets of controllers were created by modifying $\mathbf{S}_{z_c}$. Controller Set 7 has $\mathbf{z}_c$ being comprised of the actuator displacement(d) and command signal(u). Set 8 has $\mathbf{z}_c$ comprised of the actuator velocity(v) and command signal, while Set 9 is for the absolute actuator acceleration(a) and controller command signal. The trade-off curves for the structure response performance indices versus the controller effort indices are given in Figure 5. In Figure 5, we can see very dramatic changes in the performance trade-off curves. Note the change in scale from Figures 3 and 4. For low-to-medium effort levels, controller Sets 7–9 have increased the actuator displacement demands while decreasing the actuator acceleration demands. This effect is most significant in Set 9, which is the only controller set to shift the storey acceleration versus actuator acceleration curve at high levels of structural attenuation. For this controller set, increased actuator displacement demands occur at low-to-medium response attenuation, while a decrease in actuator acceleration demands is present over then entire domain. This trend suggests that including the

Table I. Simulations investigating regulated output

Set	$\mathbf{z}_s$	$\mathbf{z}_c$	ρ	J6	J7	J8	J9	J10	max(u)	max($\ddot{x}_{am}$)	max(x_m)
	Open loop			0·620	1·043	0·077	0·083	1·140	0·000	5·428	0·246
S1	d	u	12·0	0·387	0·717	1·038	1·052	0·944	0·875	4·676	3·160
S2	v	u	10·0	0·386	0·710	1·083	1·108	0·961	0·926	4·855	3·346
S3	a	u	10·0	0·388	0·702	1·063	1·117	0·996	0·910	4·849	3·283
S4	d,v	u	8·0	0·388	0·715	1·036	1·054	0·932	0·873	4·706	3·155
S5	d,a	u	8·0	0·391	0·686	1·096	1·194	1·144	0·930	5·320	3·349
S6	v,a	u	7·0	0·388	0·706	1·060	1·104	0·951	0·905	4·766	3·269
S7	d	d,u	8·0	0·386	0·707	1·070	1·105	0·869	0·943	4·185	3·370
S8	d	v,u	12·0	0·385	0·714	1·068	1·050	0·839	0·904	4·041	3·230
S9	d	a,u	8·0	0·380	0·682	1·277	1·274	0·887	1·119	3·980	3·892
S10	d	u	12·0	0·387	0·717	1·038	1·052	0·944	0·875	4·676	3·160
Set	$\mathbf{z}_s$	$\mathbf{z}_c$	ρ	J1	J2	J3	J4	J5	σ_u	$\sigma_{\ddot{x}_{am}}$	σ_{x_m}
	Open loop			0·576	0·976	0·071	0·071	1·043	0·000	1·867	0·093
S1	d	u	12·0	0·228	0·351	0·679	0·674	0·703	0·210	1·258	0·889
S2	v	u	10·0	0·221	0·339	0·705	0·699	0·722	0·220	1·292	0·924
S3	a	u	10·0	0·223	0·342	0·698	0·692	0·716	0·217	1·282	0·914
S4	d,v	u	8·0	0·229	0·351	0·678	0·673	0·702	0·210	1·257	0·889
S5	d,a	u	8·0	0·219	0·334	0·713	0·707	0·713	0·225	1·277	0·933
S6	v,a	u	7·0	0·224	0·343	0·695	0·689	0·714	0·216	1·279	0·911
S7	d	d,u	8·0	0·224	0·340	0·695	0·692	0·648	0·224	1·160	0·910
S8	d	v,u	12·0	0·231	0·351	0·670	0·664	0·621	0·215	1·112	0·878
S9	d	a,u	8·0	0·219	0·371	0·759	0·754	0·629	0·258	1·126	0·994
S10	d	u	12·0	0·228	0·351	0·679	0·674	0·703	0·210	1·258	0·889

actuator acceleration in the measure of control effort may be beneficial when the peak actuator acceleration is a primary concern. Example controller simulation results from these controller sets are also given in Table I.

Impact of model reduction

Sensitivity to the choice of when to perform model reduction was investigated by designing controllers using two methods. The first was to reduce the 28th-order evaluation model to a 10th-order model at the onset. This 10th-order system was augmented with the frequency weighting of the input filter, $\mathbf{W}_{\ddot{x}_g}$, creating a 12th-order design model. From this design model, 12th-order dynamic controllers were synthesized and evaluated. All of the results presented so far followed this approach. These and all other model reductions performed in this study used the balanced realization model reduction technique.

The second approach taken was to augment the full-order evaluation model with the frequency weighting and synthesize controllers. The resulting design model then becomes 30th-order. After the synthesis, these controllers were reduced to 12th-order controllers and simulated with the evaluation model.

Controller Set 10 was generated in this manner. The design objectives, as defined by the regulated output, for this set of controllers are identical to those of Controller Set 1, i.e. to reduce the structural displacements while measuring control cost by the controller command signal. The performance indices for one level of drift reduction can be found in Table I. The difference between the performance indices for the controller in Set 1 and the controller in Set 10 are all less than 0·2 per cent. This insignificant difference occurred repeatedly in several other similar comparisons not presented here. Thus, this investigation indicated that controller effectiveness of these controllers for the AMD model is insensitive to the choice of when to perform the necessary model reduction. Fundamentally, a 10th-, 12th-, or 28th-order model can capture the significant dynamic behaviour of the controller AMD model.

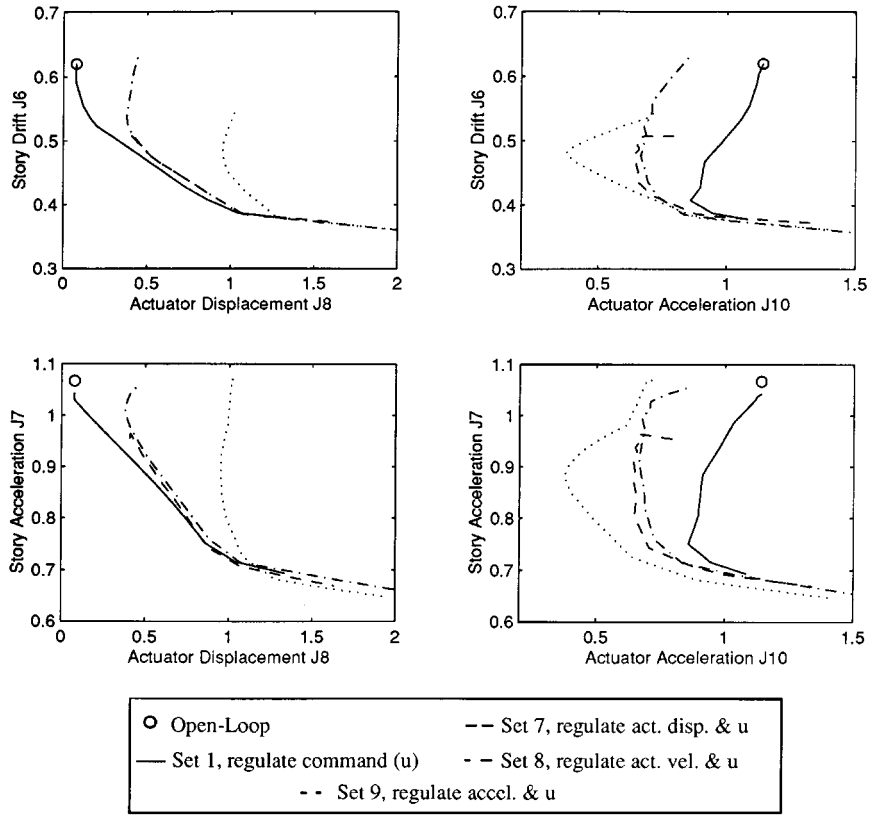

Figure 5. Investigation of $\mathbf{S}_{z_s}$, actuator effort regulation

Sensitivity of performance to available sensors

Although the example dynamic output feedback contollers presented in this research were designed using the six primary sensor measurements given in the benchmark problem, a factor of interest is the degradation of the controller performance when all of these sensors are not made available. For the examination of this effect five sets of controllers were designed using fewer than the full six sensors available in $\mathbf{y}(t)$. The base case for this comparison is the controllers from Controller Set 5 of the previous discussion, which regulates the structural displacements, structural accelerations, and the actuator command signal. From this base, controllers were designed for fewer available sensors. The combinations of sensors made available can be seen in Table II. The major result of the synthesis and simulation of the controllers is to show how insensitive the performance of the controllers is to the available sensors. Figure 6, shows the performance trade-off curves for the aforementioned six sensor case and the case where only one sensor is available to the controller, the third floor structural acceleration. Here we can see negligible change in the trade-off between structural drift and actuator displacement. Some degradation in performance occurs as measured by the peak acceleratons, J7 and J10; however, this degradation is less than 10 per cent change from the case using the full sensor arrangement. Specific performance indices of peak response for sample controllers with the peak drift index around 0·388 can be found in Table II.

Figure 7 shows two loop transfer functions from the command signal input through the plant and controller back to the command signal. The two loop transfer functions shown are for controllers from Set 5 with $\rho = 8{\cdot}0$. These cases are the six sensor and one sensor controllers for which the simulated results are

Table II. Set 5 controllers with limited sensors

Sensors in $\mathbf{y}(t)$	J6	J7	J8	J9	J10	max(u)	max($\ddot{x}_{am}$)	max(x_m)
Open loop	0·620	1·043	0·077	0·083	1·140	0·000	5·428	0·246
$x_m\ \ddot{x}_{a1}\ \ddot{x}_{a2}\ \ddot{x}_{a3}\ \ddot{x}_{am}\ \ddot{x}_g$	0·391	0·686	1·096	1·194	1·144	0·930	5·320	3·349
$x_m\ \ddot{x}_{a1}\ \ddot{x}_{a2}\ \ddot{x}_{a3}\ \ddot{x}_{am}$	0·392	0·691	1·104	1·194	1·203	0·929	5·298	3·354
$x_m\ \ddot{x}_{a3}\ \ddot{x}_{am}$	0·394	0·703	1·024	1·128	1·115	0·864	5·101	3·096
$x_m\ \ddot{x}_{a3}$	0·394	0·704	1·028	1·132	1·104	0·867	5·111	3·106
$\ddot{x}_{a3}\ \ddot{x}_{am}$	0·394	0·704	1·040	1·144	1·124	0·876	5·227	3·143
$\ddot{x}_{a3}$	0·394	0·704	1·044	1·152	1·114	0·880	5·169	3·155

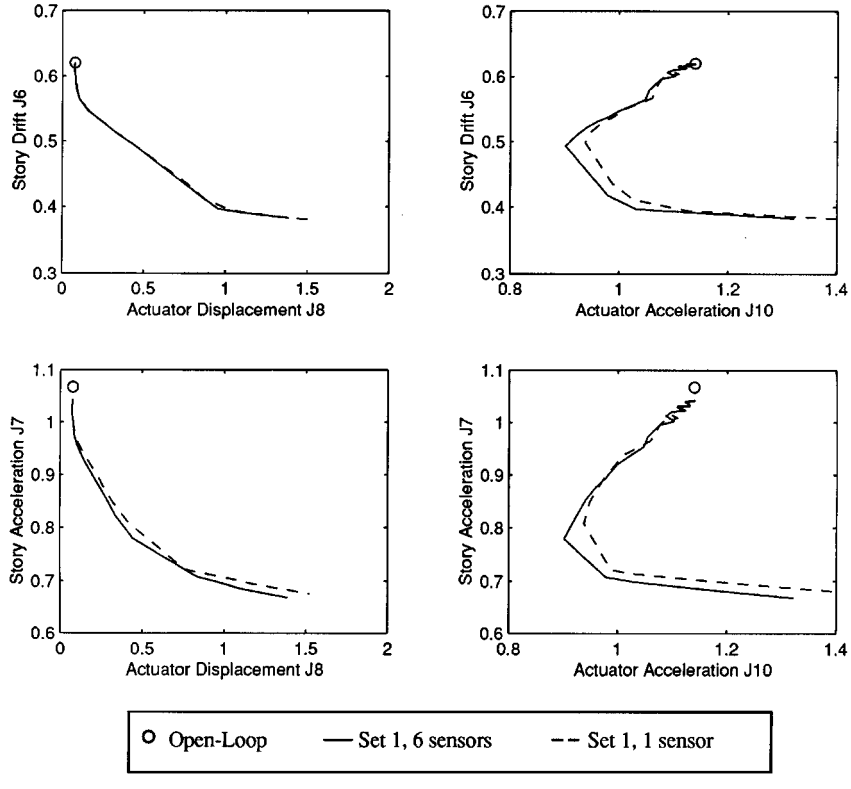

Figure 6. Effect of limited sensors

provided in Table II. Both of these loop transfer function have the desirable property of low gains at frequencies greater than 200 rad/sec, and both are highly tuned to the natural frequencies of the structures. As these controllers were designed solely for nominal performance, their robustness to variations in the natural frequency are not guaranteed. We can, however, conclude from the loop transfer plots that the single sensor controller will have a faster degradation of performance with respect to changes in the natural frequency than the six sensor case. This effects is apparent from the loop transfer gain having damped zeros located very near the tuned poles of the system. An example of how to build robustness to variations of the natural frequency into $\mathbf{H}_\infty$ methods similar to those used here can be found in Balas and Young.[13]

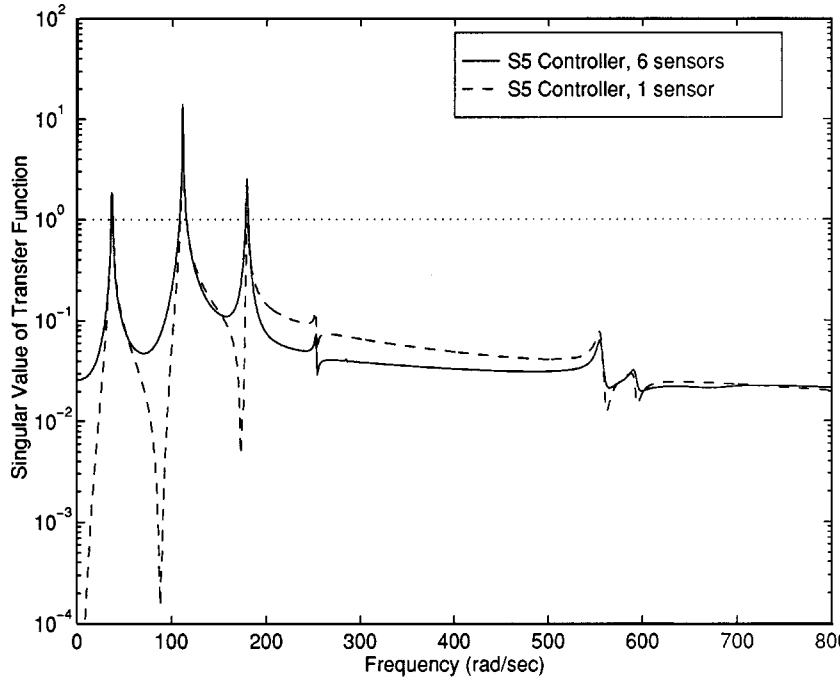

Figure 7. Example loop gain transfer function

CONCLUSIONS

This paper has developed a design model for the synthesis of $\mathbf{H}_\infty$ dynamic output feedback controllers, and applied this model to active mass driver benchmark problem posed by Spencer *et al.*[1] The example controllers designed use acceleration output feedback of the structure coupled with the additional actuator sensors and ground motion sensor. The details on the choice of regulated output for the design model have been investigated extensively. From this investigation, we recommend choosing the regulated output for design to be a combination of the structural displacements and accelerations as the measure of structural response and a combination of the actuator acceleration and command signal as the measure of control effort. The relative weights of these factors can significantly affect the actuator capacities required to achieve a desirable level of structural performance. In addition we found the controller design process for the AMD model to be insensitive to when model reduction is performed, suggesting the least computationally intensive method investigated is adequate for this type of system. Finally, the performance of the controllers with the nominal evaluation was not dramatically affected by the removal of available sensors; however this removal will significantly decrease the robustness to variations in the nominal model.

ACKNOWLEDGEMENTS

Financial support for this research was provided by the National Science Foundation Presidential Young Investigator Award No. BCS-9058316, and the Office of Naval Research (ONR) and the Naval Research Lab (NRL) Grant No. N00014-94-1-0554.

REFERENCES

1. B. F. Spencer Jr., S. J. Dyke and H. S. Deoskar, 'Benchmark problems in structural control: Part I—Active mass driver system', *Earthquake Engng. Struct. Dyn.* **27**, 1127–1139 (1998).

2. B. F. Spencer, Jr., S. J. Dyke, M. K. Sain and P. Quast, 'Acceleration feedback control strategies for aseismic protection', *ASCE J. Engng. Mech.* **120**(1), 135–158 (1993).
3. F. Jabbari, W. E. Schmitendorf and J. N. Yang, '$\mathbf{H}_\infty$ control for seismic excited buildings with acceleration feedback', *ASCE J. Engng. Mech.* **121**(9), 994–1001 (1995).
4. S. J. Dyke, B. F. Spencer, P. Quast, M. K. Sain, D. C. Kaspari and T. T. Soong, 'Acceleration feedback control of MDOF structures', *ASCE J. Engng. Mech.* **122**(9), 907–917 (1996).
5. J. G. Chase, H. A. Smith and T. Suzuki, 'Robust $\mathbf{H}_\infty$ control considering actuator saturation Part 2: applications', *ASCE J. Engng. Mech.* **122**(10), 984–993 (1996).
6. G. Gu and P. Mishra, 'Disturbance attenuation and $\mathbf{H}_\infty$ optimization with linear output feedback control', *J. Guidance, Control, Dyn.* **17**(1), 145–152 (1994).
7. P. L. D. Peres, J. C. Geromel and S. R. Souza, '$\mathbf{H}_\infty$ robust control by static output feedback', *Proc. 1993 American Control Conf.* San Francisco, CA, June 1993, pp. 620–621.
8. I. E. Kose, W. E. Schmitendorf, F. Jabbari and J. N. Yang, '$\mathbf{H}_\infty$ active seismic response control using static output feedback', *ASCE J. Engng. Mech.* **122**(7), 651–659 (1996).
9. R. E. Skelton, J. Stoustrup and T. Iwasaki, 'The $\mathbf{H}_\infty$ control problem using static output feedback', *Int. J. Robust Nonlinear Control* **4**, 449–455 (1994).
10. J. C. Doyle, K. Glover, P. P. Khargonekar and B. A. Francis, 'State-space solutions to standard $\mathbf{H}_2$ and $\mathbf{H}_\infty$ control problems', *IEEE Trans. Automat. Control* **34**(8), 831–847 (1989).
11. S. P. Boyd, L. el Ghaoui, E. Feron and V. Balakrishnan, *Linear Matrix Inequalities In System And Control Theory*, Vol. 15 of *Studies In Applied Mathematics*, SIAM, Philadelphia, PA, 1994.
12. M. A. Rotea and R. K. Prasanth, 'An interpolation approach to multiobjective $\mathbf{H}_\infty$ design', *Int. J. Control* **65**(4), 699–720 (1996).
13. G. J. Balas and P. M. Young, 'Control design for variations in structural natural frequencies', *AIAA J. Guidance, Dyn. Control* **18**(2), 325–332 (1995).
14. J. Stoustrup and H. H. Niemann, 'The general $\mathbf{H}_\infty$ problem with static output feedback', *Proc. American Control Conf.*, San Francisco, CA, June 1993, pp. 600–604.

